Journal of Applied Electrochemistry **34**: 1119–1125, 2004.

Preparation of rechargeable lithium batteries with poly(methyl methacrylate) based gel polymer electrolyte by *in situ* γ-ray irradiation-induced polymerization

Y.F. ZHOU[1,2], S. XIE[1], X.W. GE[1], C.H. CHEN[1]* and K. AMINE[3]
[1]*Department of Materials Science and Engineering, University of Science and Technology of China, Anhui, Hefei 230026, P.R. China*
[2]*School of Chemistry and Chemical Engineering, Anhui University, Anhui, Hefei 230039, P.R. China*
[3]*Argonne National Laboratory, Chemical Technology Division, 9700 S. Cass Avenue, Argonne, IL 60439, USA*
*(*author for correspondence, e-mail: cchchen@ustc.edu.cn)*

Received 11 November 2003; accepted in revised form 6 June 2004

Key words: gel polymer electrolyte, lithium ion batteries, PMMA, γ-ray irradiation induced polymerization

Abstract

An admixture of commercial liquid electrolyte (LB302, 1 M solution of $LiPF_6$ in 1:1 EC/DEC) and methyl methacrylate (MMA) was enclosed in CR2032 cells. The assembled cells were then γ-ray-irradiated using configurations of half cells and full cells. Through this *in situ* irradiation polymerization process, we obtained rechargeable lithium ion cells with poly(methyl methacrylate) (PMMA) based gel polymer electrolytes (GPE). Galvanostatic cycling, AC impedance spectroscopy, and cyclic voltammetry were employed to investigate the electrochemical properties of the cells and the gel polymer electrolyte. This PMMA-based gel polymer electrolyte was found to exhibit a high ionic conductivity (at least 10^{-3} S cm^{-1}) at room temperature. Due to a significant increase in the charge transfer resistance between the GPE and the cathode, the cell impedance of a PMMA-based lithium ion cell is greater than that of a liquid-electrolyte-based cell. The discharge capacity of a $LiNi_{0.8}Co_{0.2}O_2$/GPE/graphite is approximately 145 mAh g^{-1} for the first cycle and decreases to123 mAh g^{-1} after 20 cycles. In addition, a large initial cell impedance (LICI) was observed in the irradiated positive half cell. In this paper, we propose a possible mechanism related to the detachment of the PMMA layer from the lithium electrode. This detachment of the PMMA layer from the lithium electrode has not been explicitly discussed previously.

1. Introduction

Polymer electrolytes can be classified into two categories: solid polymer electrolyte (SPE) and gel polymer electrolyte (GPE). Lithium batteries with SPEs are not subject to the problem of electrolyte leakage, but exhibit lithium ion conductivities that range from 10^{-8} to 10^{-5} S cm^{-1} at room temperature, which is not sufficient for practical battery applications. Lithium ion batteries with liquid electrolyte have conductivities above 10^{-3} S cm^{-1} at 25 °C and can thus operate very nicely at room temperature, but may be subject to electrolyte leakage. Thus, lithium batteries with GPEs, combine the best features of both SPE and liquid electrolyte types of batteries and have none of the disadvantages of either. They thus represent a new type of lithium-ion battery with great potential to dominate the market for rechargeable batteries [1–5].

PMMA gel polymer electrolytes exhibit high conductivities and good electrochemical stability; where their electrochemical stability window is up to 4.5 V (vs Li/Li^+) [6, 7]. GPEs are normally prepared by first dissolving PMMA in a liquid electrolyte at a temperature above 60 °C, then forming electrolyte composite films by gel casting or immersing the porous separators into the hot gel electrolyte solution, and finally cooling the films to room temperature [2, 5–10]. The electrode laminates are prepared in a similar manner. The gel-polymer separator electrolyte film is then combined with the electrode laminates to assemble a complete battery. This fabrication technique is complicated, and all the steps must be performed in a dry, oxygen-free atmosphere. Furthermore, a relatively high mechanical strength is required for the polymer films, and this is difficult to achieve when one uses this fabrication approach. Therefore, it is desirable to conduct the polymerization process in an assembled cell.

In our previous work, rechargeable lithium ion cells with PMMA-based gel polymer electrolyte were fabricated through *in situ* thermal polymerization (Y.F. Zhou, submitted for publication), which has two shortcomings. First, an initiator must be used, which leads to a more complicated cell chemistry. Second, polymerization is usually not complete under the available thermal conditions. Residual monomers from thermal polymerization may thus adversely influence the electrochemical

properties of the batteries. On the other hand, polymerization induced by high-energy irradiation is a well-established technique and does not require any initiators. This technique thus has many advantages, such as the fact that the polymerization proceeds mildly and thoroughly, the chemistry of the reaction system is free of contamination, and the energy consumption is relatively low. The radiation types that have been used in the polymerization process include ultraviolet (UV), electronic beam, and γ radiation. UV rays have the lowest energy and have only very limited penetration capabilities, whereas γ rays have the highest energy and can penetrate almost any material including the cell can enclosure. In addition, polymerization initiation by means of γ radiation is very efficient. Therefore, γ radiation from Co-60 is commonly used in the polymerization process [11].

Several studies describe GPEs prepared by irradiation polymerization with UV, electronic beam, or γ-ray sources [12, 13]. In these studies, however, the polymerization processes were conducted out of cell prior to cell assembly. In our studies, the methyl methacrylate (MMA) monomer is mixed with liquid electrolyte to form a liquid precursor so the batteries can be assembled by the relatively simple technology used for conventional liquid electrolyte lithium ion batteries, followed by γ-ray irradiation of the assembled cells to obtain gel polymer type cells. PMMA alone has rarely been used as the polymer matrix of the cell electrolyte [4, 8] because the mechanical strength of a PMMA layer is so low that it requires very careful handling during cell preparation. Our *in situ* polymerization approach does not require a high mechanical strength in order for the polymer matrix to immobilize the liquid electrolyte.

2. Experiment

MMA monomer (99.0%) was dehydrated with CaH_2 and then purified further by vacuum distillation. The purified MMA was blended with a commercial liquid electrolyte (LB302, 1 M $LiPF_6$ in 1:1 EC/DEC) in a mass ratio of 1:4 MMA/LB302 to form the precursor solution for the gel polymer electrolyte. CR2032 coin cells were fabricated using this blend as the liquid electrolyte, a porous separator (Celgard 2400) with configurations of $LiNi_{0.8}Co_{0.2}O_2$/Li, graphite/Li, and $LiNi_{0.8}Co_{0.2}O_2$/graphite. The $LiNi_{0.8}Co_{0.2}O_2$ laminate consisted of 84 wt % $LiNi_{0.8}Co_{0.2}O_2$, 8 wt % acetylene black, and 8 wt % polyvinylidene fluoride (PVDF) and the graphite laminate consisted of 91 wt % graphite and 9 wt % PVDF and were provided by Argonne National Laboratory. The load densities of the active materials were 9 mg cm^{-2} for the positive electrode and 5.8 mg cm^{-2} for the graphite negative electrode. These cells were placed in a chamber with a Co-60 γ irradiation source whose irradiation dose rate at different cell positions was calculated at regular time intervals. Cells were placed at a position with a dose rate of 138.9 Gy min^{-1}. After 14 h of irradiation, the MMA in the electrolyte was polymerized, forming a GPE.

In order to determine a suitable polymer content and irradiation time, solutions with different MMA/LB302 mass ratios ranging from 0 to 1:4 were sealed in glass bottles that were then subjected to γ irradiation for varying time periods. After irradiation, the degree of polymerization of the solutions, especially their viscosity changes, was examined. In addition, the precursor solutions were sealed in stainless steel (SS) CR2032 coin cell with a cell configuration of stainless steel (SS)/porous separator (LB302 + MMA drenched)/SS. The degree of electrolyte polymerization in these cells was examined by disassembling them after they had been subjected to various levels of γ irradiation. Because γ-rays, especially those emitted from a Co-60 source, can penetrate nearly any material [11], the glass bottles (2 mm thick) and stainless steel cans (1 mm thick) used in this study can receive sufficient doses of radiation to initiate polymerization. The ionic conductivity of the GPE was measured with SS/GPE/SS cells by means of AC impedance spectroscopy under 50 mV amplitude and a frequency range of 0.001–100 kHz. Cyclic voltammetry of $LiNi_{0.8}Co_{0.2}O_2$/MMA:LB302(1:4)/Li and graphite/MMA:LB302(1:4)/Li cells before and after γ irradiation were measured with a scan rate of 0.1 mV s^{-1}. For comparison, similar half cells with only LB302 as the electrolyte also were measured. All the measurements were performed with an electrochemical workstation (model CHI 604A). In addition, the irradiated cells (half cells and full cells) were cycled on a multichannel battery cycler (Neware BTS-610) with a current density of 0.2 or 0.06 mA cm^{-2}. Low current densities were used in these studies because the impedance of the GPE-positive half cells and full cells are large. Therefore, a small current density of 0.06 mA cm^{-2} was chosen for these high impedance cells.

3. Results and discussion

In the experiments to determine a suitable ratio of MMA and liquid electrolyte, it was found that when the mass ratio of MMA: LB302 $\leqslant$ 1.0:4.0, the liquid electrolyte could not be immobilized because the content of the polymer PMMA was too small. Hence, in order to immobilize the liquid electrolyte and form the GPE, the mass ratio of MMA:LB302 needs to be controlled in the range of 1.0:2.0 to 1.0:4.0. Under these conditions the suitable polymerization time to form a GPE is about 14 h.

Figures 1 and 2 show the charge–discharge property of a $LiNi_{0.8}Co_{0.2}O_2$/GPE/Li cell (Figure 1) and a Graphite/GPE/Li cell (Figure 2). In the positive half cell (Figure 1), at the beginning of the first charge step, the cell voltage reaches about 4.2 V and then rapidly drops to about 3.9 V, which was then followed by the usual charging process. Obviously, the initial cell impedance is rather large but was greatly reduced in a short time. In fact, an irradiated positive half cell usually

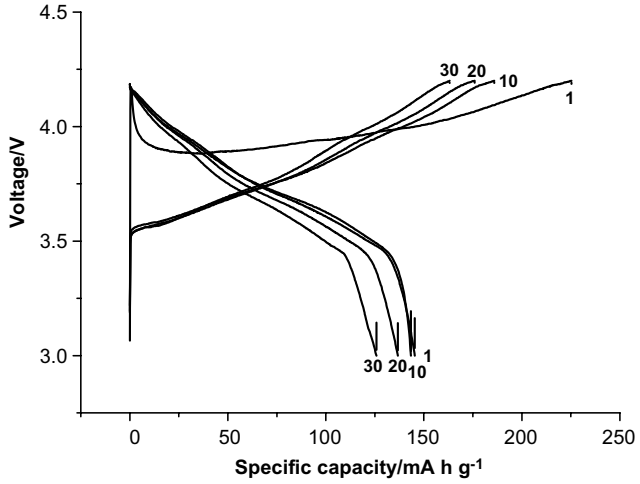

Fig. 1. The cycling characteristics of cell $LiNi_{0.8}Co_{0.2}O_2$/GPE/Li at a current density of 0.06 mA cm^{-2}. The GPE was prepared with MMA/LB302 = 1/4 and irradiated at 138.9 Gy min^{-1} for 14 h. Voltage range: 3.0–4.2 V.

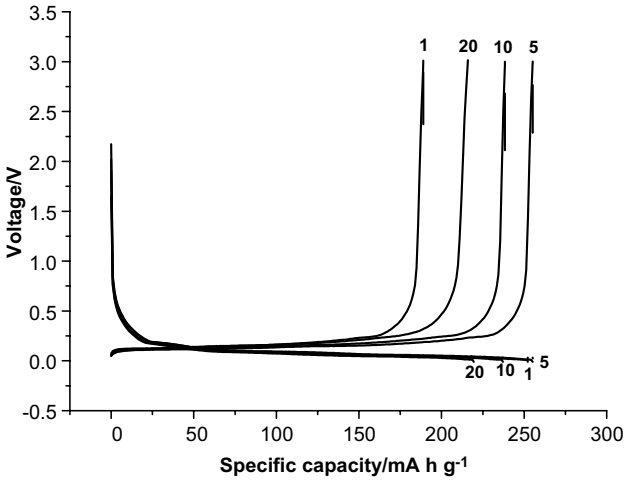

Fig. 2. The cycling characteristics of the graphite/GPE/Li cell at a current density of 0.2 mA cm^{-2}. The GPE was prepared with MMA/LB302 = 1/4 and irradiated at 138.9 Gy min^{-1} for 14 h. Voltage range: 0–3 V.

goes through up to a dozen rapid constant-current cycles before its charge–discharge exhibits the behavior shown in Figure 1. These cycles act as a formation process for the cell. As shown in Figure 3, in contrast to cells with a lithium metal anode, the phenomenon of large initial cell impedances (LICI) and a needed formation process are not observed in full cells with graphite anodes. Therefore, the LICI must be related to the metallic lithium anode. Presumably, an insulating PMMA film is formed on the lithium metal surface during irradiation. This film may be detached at the beginning of the charge step, during which the lithium is deposited on the surface of the lithium electrode, leading to a decrease in cell impedance during the first charging process. In subsequent charge–discharge cycles, the cells reach normal capacity and possess electrochemical characteristics similar to those observed in a $LiNi_{0.8}Co_{0.2}O_2$/LB302/Li cells. For the negative half cell, the charge (i.e., delithiation) capacity is relatively low (about 180 mAh g^{-1}) during the first cycle, but increases to 260 mAh g^{-1} after three cycles. In subsequent cycles, the capacity fade follows a pattern similar to that of a negative half cell with liquid electrolyte. The reason for the small first-cycle capacity may also be related to the PMMA film on the lithium electrode that is responsible for the LICI phenomenon mentioned above.

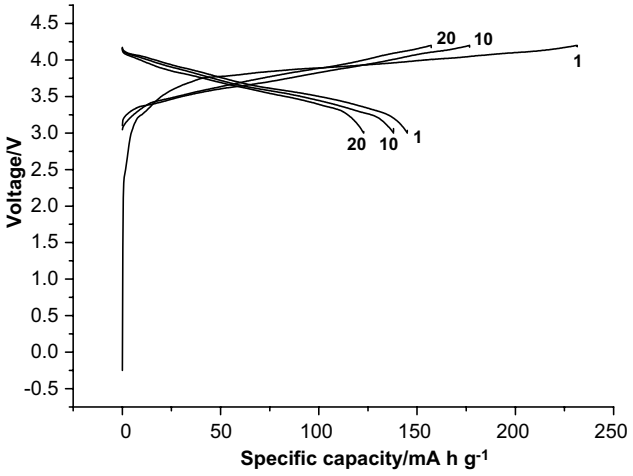

Fig. 3. The cycling characteristics of cell $LiNi_{0.8}Co_{0.2}O_2$/GPE/graphite at a current density of 0.06 mA cm^{-2}. The GPE was prepared with MMA/LB302 = 1/4 that was irradiated at 138.9 Gy min^{-1} for 14 h. Voltage range: 3.0–4.2 V.

Figures 3 and 4 show the charge–discharge characteristics of two full cells: a $LiNi_{0.8}Co_{0.2}O_2$/GPE(1:4 PMMA:LB302)/graphite cell (Figure 3) and a $LiNi_{0.8}Co_{0.2}O_2$/LB302/graphite cell (Figure 4). The LICI phenomenon disappears in Figure 3. The first charge capacity of the GPE cell reaches 230 mAh g^{-1}, while that of the LB302 cell is about 200 mAh g^{-1}. This difference is probably due to the different current densities applied to the cells, i.e., 0.06 mA cm^{-2} to the GPE cell and 0.2 mA cm^{-2} to the LB302 cell (Figure 4).

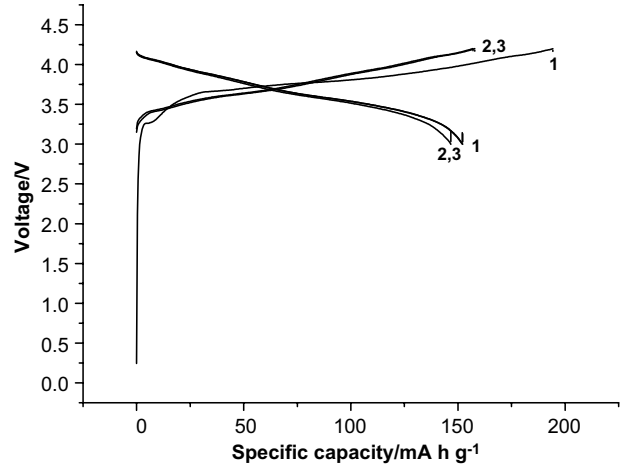

Fig. 4. The cycling characteristics of cell $LiNi_{0.8}Co_{0.2}O_2$/LB302/graphite at a current density of 0.2 mA cm^{-2}. Voltage range: 3.0–4.2 V.

On the other hand, their discharge capacities are all close to 150 mAh g^{-1}. This relatively large capacity fade during the first cycle (50–80 mAh g^{-1}) is characteristic of a $LiNi_{0.8}Co_{0.2}O_2$ electrode [14, 15], which is related to the highly oxidative nature of Ni^{4+} in the fully charged cathode material. Furthermore, such a capacity fade is composed of two parts, i.e., the irreversible and the reversible [16]. Figures 3 and 4 illustrate that the reversible capacity fade of the cells is about 3 mAh g^{-1} per cycle for the GPE cell and about 10 mAh g^{-1} for the LB302 cell. Considering the different current densities applied, the similar discharge capacity suggests that the impedance of the GPE cell is higher than that of the LB302 Cell. Impedance spectra measurements of both cells (Figure 5A and B) confirm the significant difference in cell impedance. It is clear that the biggest difference lies in the semicircle in the medium-frequency (0.05–70 Hz) range. According to the symmetric cell studies by Chen et al. [17, 18], this semicircle may be attributed mainly to the charge-transfer processes within the $LiNi_{0.8}Co_{0.2}O_2$ cathode. As shown in Figure 6, the ionic conductivity of the PMMA-based GPE is above

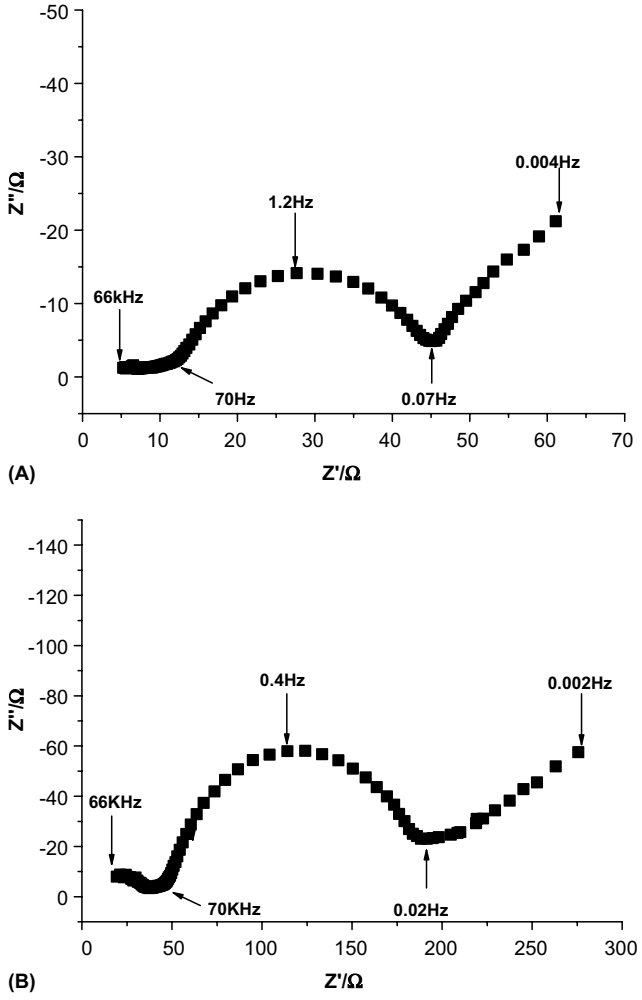

Fig. 5. (A) AC impedance spectra of a $LiNi_{0.8}Co_{0.2}O_2$/LB302/graphite cell and (B) the $LiNi_{0.8}Co_{0.2}O_2$/GPE/graphite cell impedance spectra after three formation cycles. The frequency range was 0.001–100 kHz, electrode area 1.54 cm^2 (OCV = 4.0 V).

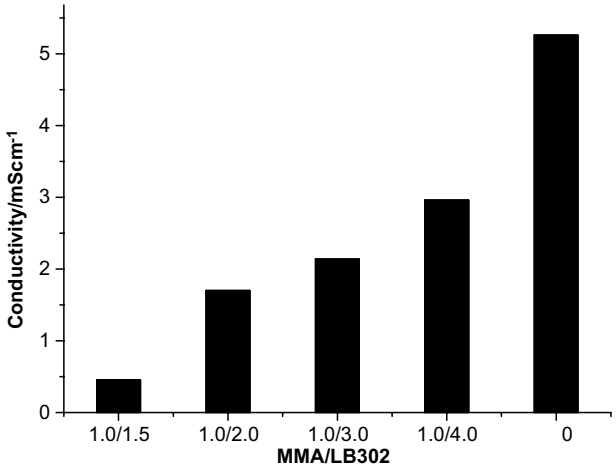

Fig. 6. The relationship between the ionic conductivity of the GPE and the MMA/LB302 composition. All samples were irradiated at 138.9 Gy min^{-1} for 14 h.

2×10^{-3} S cm^{-1}, the same order of magnitude as for LB302, with an ionic conductivity of 5.2×10^{-3} S cm^{-1}. Therefore, a PMMA film must have been formed on the cathode surface in the GPE cell, thus leading to the substantial increase in charge-transfer impedance.

Figure 7 shows the cyclic voltammograms of $LiNi_{0.8}Co_{0.2}O_2$/GPE/Li half cells before and after γ-ray irradiation (Figure 7A and B) and a $LiNi_{0.8}Co_{0.2}O_2$/ LB302/ Li half cell for comparison (Figure 7C). Apparently, except for the difference in peak positions and intensity, these three voltammograms exhibit similar lithium insertion and extraction processes, each of which consists of three steps. This is also in agreement with results for liquid electrolyte cells [19–21]. Because no additional peak is observed in the first cycle for the MMA- or the PMMA-containing cells (Figure 7A and B), it appears that no significant oxidation or reduction of the MMA monomers or oligomers can be detected, suggesting that the addition of MMA should not consume the active lithium on the cathode side. However, we cannot exclude the possibility that the MMA monomers may be reduced to form a ketol at the interface between the electrolyte and the lithium when the cell is assembled and before the formation of a dense SEI layer on the lithium electrode (see below).

Figure 8A–C shows the cyclic voltammograms of graphite/GPE/Li half cells before and after γ-ray irradiation (Figure 8A and B) and a graphite/LB302/Li half cell for comparison (Figure 8C). In the MMA-containing cell (Figure 8A), it can be seen that, in addition to the reduction peak at about 0.6 V that is believed to be responsible for the formation of the solid electrolyte interface (SEI) layer (peak a) [22], there is an extra irreversible reduction peak (peak b) with an onset potential at 1.5 V and a peak potential at 1.0 V during the first lithiation step. This extra peak can be explained by ester reduction reactions of the MMA monomer. A possible reduction scenario to produce a ketol type material [23] is shown below:

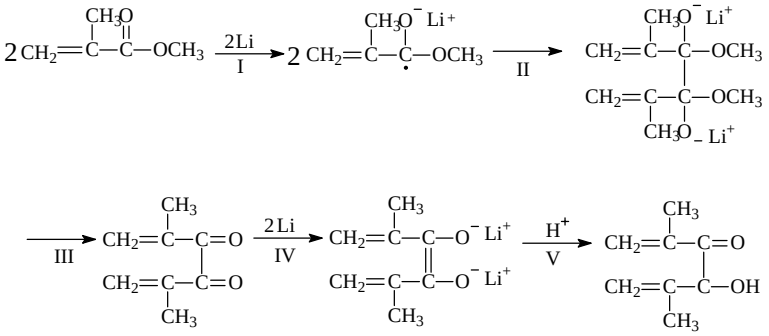

The proton (H^+) at step V may come from HF generated in the electrolyte. The reaction pathways demonstrated in the above reactions involve two reduction steps (I and IV). Therefore, the peak b in Figure 8A should be the overall result of two single-electron reactions. This is also why the difference between the peak potential E_p (ca. 1.05 V) and its half-peak potential $E_{p/2}$ (ca. 1.15 V) is significantly greater than 56.5 mV, which is for one single-electron reaction [24]. However, after the formation of the SEI layer (peak a in Figure 8A), MMA dissolved in the solvent is isolated from electrons from the graphite anode, leading to the termination of this reduction reaction. Therefore, this peak is not observed in the subsequent cycles. On the other hand, this peak is not observed in the first cycle of the PMMA half cell (Figure 8B); implying that nearly all of the MMA monomers have been polymerized during the γ-ray irradiation. In addition, all three cyclic voltammograms exhibit similar lithium insertion or extraction processes, but the peak intensities of MMA- or PMMA-containing cells (Figure 8A and B) are much

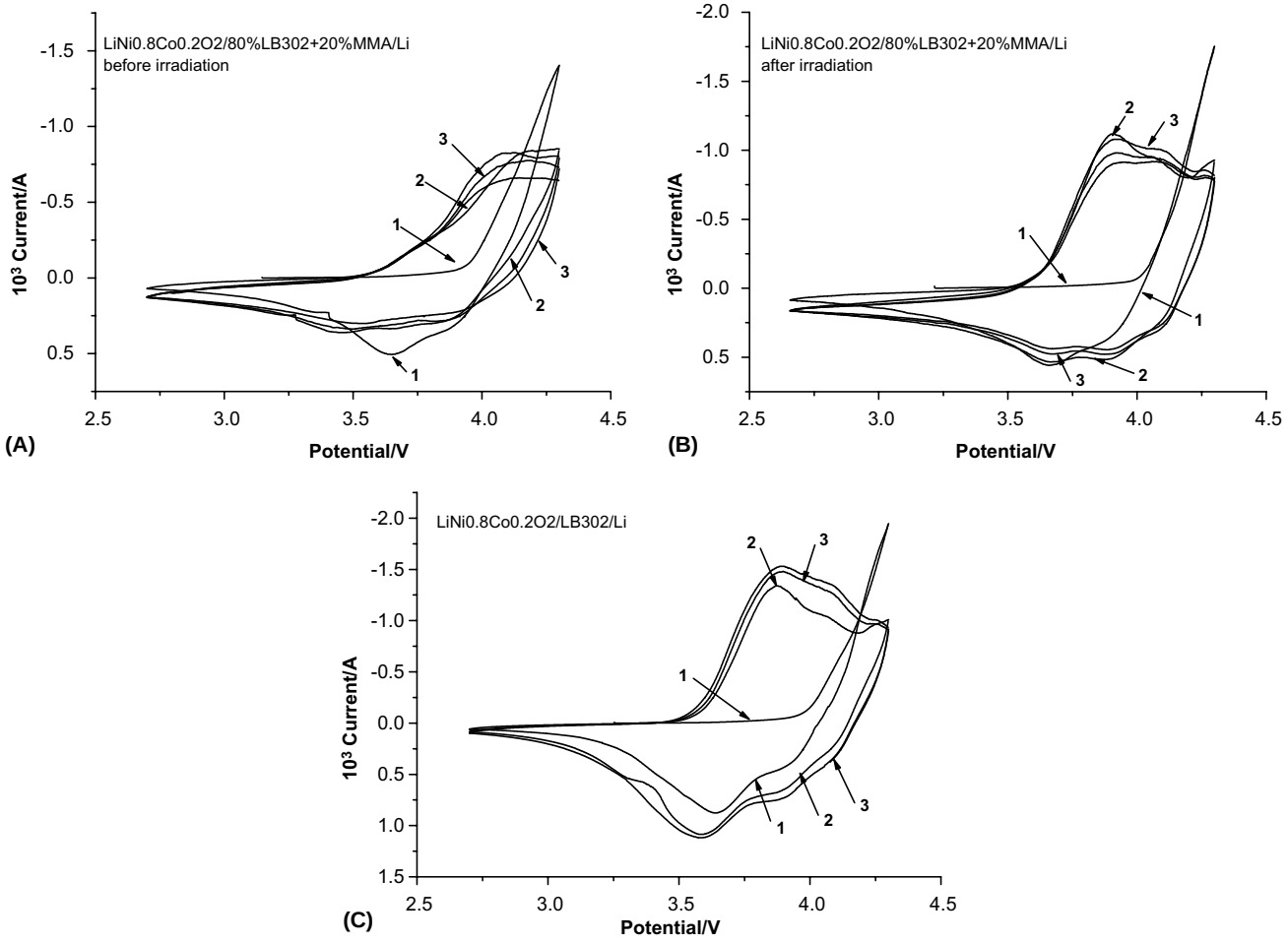

Fig. 7. Cyclic voltammetry characteristics of positive half cells: $LiNi_{0.8}Co_{0.2}O_2$ /80%LB302 + 20%MMA/Li, before irradiation (A) and after irradiation (B) and $LiNi_{0.8}Co_{0.2}O_2$/LB302/Li (C). Potential scan rate: 0.1 mV s^{-1}.

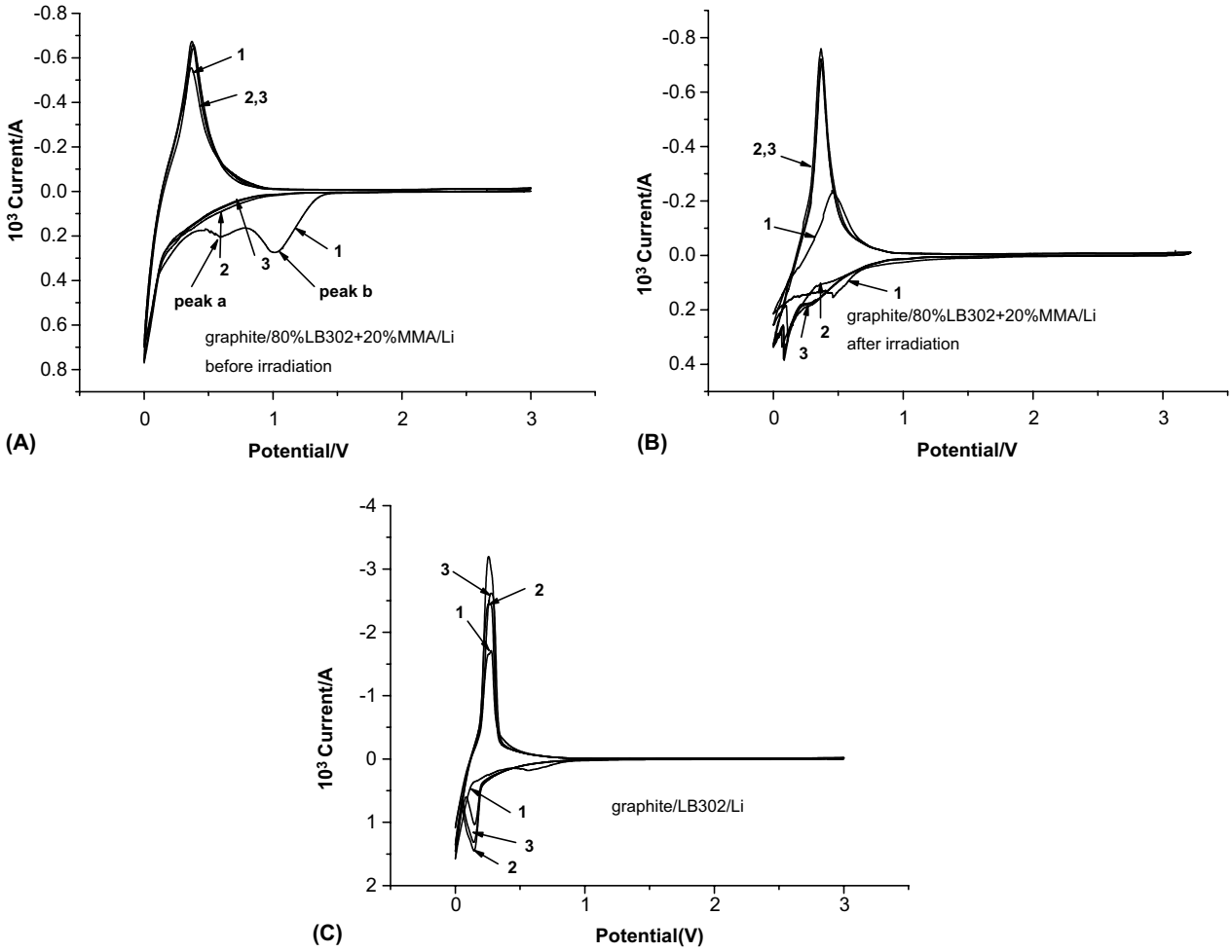

Fig. 8. Cyclic voltammetry characteristics of negative half cells: graphite/80%LB302 + 20%MMA/Li, before irradiation (A) and after irradiation (B) and graphite/LB302/Li (C). Potential scan rate: 0.1 mV s^{-1}.

weaker than those of the LB302-containing cell (Figure 8C). This difference again indicates that the impedance of an MMA- or PMMA-containing cell is significantly larger than that of an LB302-containing cell.

Looking carefully at Figure 8B, we also notice that the cathodic peak area of the first cycle is smaller than those obtained in the subsequent cycles. This is consistent with the results of capacity measurement of the graphite/Li half cell (Figure 2). From these results, it can be seen that this new approach to *in situ* fabrication of a GPE can result in GPE-based lithium ion batteries with good electrochemical performance. The discharge capacity of the GPE cell is 145 mAh g^{-1}, and it still retains 123 mAh g^{-1} after 20 cycles. Both values are quite competitive compared with those of currently commercial $LiCoO_2$/C cells with a liquid electrolyte. Although the cycling efficiency of the PMMA-based GPE cells is smaller than that of the $LiNi_{0.83}Co_{0.17}O_2$/C cells with a poly(acrylonitrile-co-methyl-ethacrylate-co-styrene) (PAMS)-based electrolyte [1], we expect that further optimization of the electrode material screening and polymer system will further improve the electrochemical performance. It should be noted here that our *in situ* approach can be extended easily to polymer systems other than PMMA.

4. Conclusions

Rechargeable lithium ion batteries with PMMA-based GPE can be fabricated through a one-step *in situ* γ irradiation process. The process is to irradiate preassembled cells containing an admixture of liquid electrolyte (LB302) and MMA at their fully discharged states. The ionic conductivity for the GPE with MMA/LB302 ratio range of 1.0/2.0–1.0/4.0 is all above 10^{-3} S cm^{-1} at room temperature. When metallic lithium is used as the anode, as in the case of $LiNi_{0.8}Co_{0.2}O_2$/GPE/Li cells, a LICI phenomenon is observed; a possible mechanism involving the detachment of a PMMA film from the lithium anode is proposed as the cause. This LICI phenomenon disappears when graphite is used as the anode. In addition, a large charge-transfer impedance between the cathode and the GPE has been observed. After the first charge–discharge cycle, the cycling performance of a GPE-based cell is good; although its specific capacity

is a little lower than that of a liquid-electrolyte-based cell at the same current density.

Acknowledgements

This study was supported by the 100 Talents Program of Academia Sinica and US Department of Energy. We are also grateful to National Science Foundation of China (Grant No. 50372064) and National Education Council of China (Grant No. 20030358057).

References

1. D.W. Kim, *J. Power Sources* **76** (1998) 175.
2. D.W. Kim, B. Oh, J.H. Park and Y.K. Sun, *Solid State Ion.* **138** (2000) 41.
3. Y. Wang, J. Travas-Sejdic and R. Steiner, *Solid State Ion.* **148** (2002) 443.
4. S.A. Agnihotry, Pradeep and S.S. Sekhon, *Electrochim. Acta* **44** (1999) 3121.
5. A.M. Stephan, R. Thirunakaran, N.G. Renganathan, V. Sundaram, S. Pitchumani, N. Muniyandi, R. Gangadharan and P. Ramamoorthy, *J. Power Sources* **81–82** (1999) 752.
6. H.J. Rhoo, *Electrochim. Acta* **42** (1997) 1571.
7. C.S. Kim and S.M. Oh, *J. Power Sources* **109** (2002) 98.
8. T. Tatsuma, M. Taguchi and N. Oyama, *Electrochim. Acta* **46** (2001) 1201.
9. N.S. Choi and J.K. Park, *Electrochim. Acta* **46** (2001) 1453.
10. T. Osaka, T. Momma, H. Ito and B. Scrosati, *J. Power Sources* **68** (1997) 392.
11. A. Charlesby, *Atomic Radiation and Polymers* (Pergamon, 1960), p. 53.
12. Y. Matsuda, N. Namegaya, *J. Power Sources* **81–82** (1999) 762.
13. Chinese patent no. CN 1315752A.
14. J.R. Ying, C.R. Wan and C.Y. Jiang, *J. Power Sources* **102** (2001) 162.
15. G.X. Wang, J. Horvat, D.H. Bradhurst, H.K. Liu and S.X. Dou, *J. Power Sources* **85** (2000) 279.
16. R. Yazami and Y.F. Reynier, *Electrochim. Acta* **47** (2002) 1217.
17. C.H. Chen, J. Liu and K. Amine, *Electrochem. Commun.* **3** (2001) 44.
18. C.H. Chen, J. Liu and K. Amine, *J. Power Sources* **96** (2001) 321.
19. Y.M. Choi and S.I. Pyun, *Solid State Ion.* **99** (1997) 173.
20. G.T.K. Fey, J.G. Chen, V. Subramanian and T. Osaka, *J. Power Sources* **112** (2002) 384.
21. S.T. Yang, J.H. Jia, L. Ding and M.C. Zhang, *Electrochim. Acta* **48** (2003) 569.
22. S. Mori, H. Asahina, H. Suzuki, A. Yonei and K. Yokoto, *J. Power Sources* **68** (1997) 59.
23. D. Barton and D. Ollis, *in* I.O. Sutherland (Ed), *Comprehensive Organic Chemistry*, Vol. 2 (Pergamon, 1979), p. 934.
24. A.J. Bard and L.R. Faulkner, *Electrochemical Methods*: *Fundamentals and Applications*, 2nd edn (John Wiley and Sons, 2001), p. 231.